POLITECNICO
MILANO 1863

SCUOLA DI INGEGNERIA INDUSTRIALE
E DELL'INFORMAZIONE

Executive Summary of the Thesis

Experimental Investigation of a Turbulent Boundary Layer Flow over a Backward-Facing Ramp

Master's Degree in Aeronautical Engineering - Ingegneria Aeronautica

Author: Andrea De Vincenzo

Advisor: Prof. Alex Zanotti

Co-advisor: Prof. Dr. Andreas Schröder

Academic year: 2023-2024

1. Introduction

The development of a new aircraft is a complex process that needs extensive preliminary analysis before any construction or flight testing. This analysis requires a robust interaction between wind tunnel experiments and computer simulations. However, the modeling of separated flow regions underneath turbulent or transitional shear flows are still quite challenging, due to their inherent complexity. Separated turbulent flow are commonly observed in both research and industrial aerodynamics applications, including wings, spoilers, turbines and car bodies. Their accurate characterization is essential, as they significantly affect the overall aerodynamic performance. As part of the DLR Göttingen internal project ADaMant [1], this work aims at providing data in order to improve the reliability and accuracy of turbulence models used in the simulation of complex aeronautical flows, specifically within the context of Reynolds-Averaged Navier-Stokes (RANS) equations. The flow solver in development is part of an effort spread between Airbus, ONERA and DLR, to compute full aircraft configurations, so advanced simulation tools that improve the design and efficiency of airplanes. Additionally, the dataset produced in this study contributes to enhance the understanding of turbulence dynamics in free shear layers. In pursuit of this, a three-dimensional, time-resolved experimental investigation of a turbulent boundary layer developing over a flat plate is conducted in the region downstream of a backward facing ramp. The Shake-The-Box technique (STB) [2], coupled with advanced data assimilation methods, is the choice for providing a large amount of high-quality data.

2. Experimental setup

The water tunnel experiments were carried out at *Große Wasserkanal Braunschweig* (GWB), a closed-circuit tunnel characterized by a test section that is 6.0 m long, 1.0 m wide, and 1.0 m high. Measurements were performed on a backward-facing ramp, as shown in Figure 1. With a step height of 8 mm, the 25 ° BFR model targets a ratio $h/\delta_{99} \approx 0.4$ at $x_h = 1.134$ m, where δ_{99} is the thickness of the boundary-layer at the edge, but in the absence of the ramp itself. The model was constructed from anodized aluminum and designed with an interchangeable insert to be studied via the STB and Temperature-Sensitive-Paint (TSP). For the STB campaign,

the insert consisted of a central glass extending over the step, with horizontal and vertical dimensions of 250 *mm* and 150 *mm*, respectively. It stood vertically in the measuring section, secured to the walls at both the top and bottom, and the body was equipped with pressure tabs, characterized by an orifice diameter of 8 *mm*. Five high-speed cameras (Phantom v2640) with 100 *mm* lenses were placed on the side of the test section, recording ORGASOL® 2002 D NAT 1 particles illuminated by a Photonics Industries DM200 Dual Head Nd:YAG laser. The measurement volume spanned approximately 80 x 90 x 20 mm^3 and was divided into two spatial subvolumes to increase the volumetric particle density. Chunk mode was used to ensure statistical convergence, with three runs recorded as time-resolved datasets. The cameras recorded at repetition rates of up to 15 kHz (7.5 kHz per subvolume). Four different velocities were tested in order to achieve Re_{xh} spanning from 1.2×10^6 to 2.7×10^6.

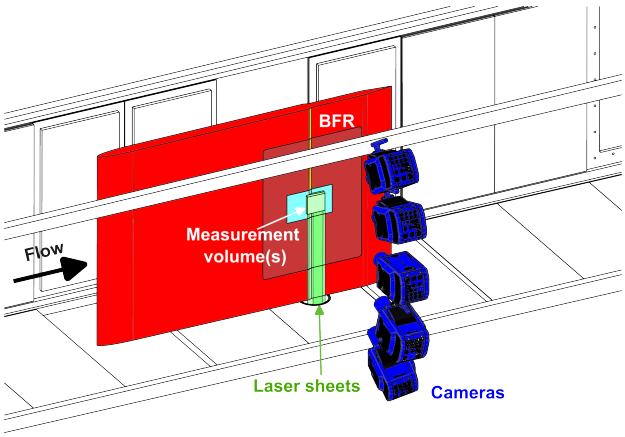

Figure 1: Schematic of the 3D measurement.

3. Results

In the following section, the results for Re =1.2×10^6 will be provided. Binning average technique was used to extract flow statistics, with a convergence analysis that was conducted beforehand.

3.1. Convergence Analysis

The statistical evaluation of the 3D flow characterization is based on time- and spanwise-averaged statistics assuming statistically steady 2D flow conditions. A binning approach was employed to extract mean statistics from data acquired in chunk mode, producing a large number of discrete, statistically independent, short-time-resolved particle trajectories. Five representative points were considered into the analysis, reflecting different flow characteristics:

- *Point 1*: Inflow condition.
- *Point 2*: Separated shear layer.
- *Point 3*: Upper recirculation region.
- *Point 4*: Near-wall reverse flow.
- *Point 5*: Maximum Reynolds stresses.

Two different grids were considered. *Grid 1* used square bins ($\Delta x = \Delta y = 126.5$ μm), suitable for capturing Reynolds stresses. *Grid 2* featured elongated bins ($\Delta x = 400$ μm, $\Delta y = 20$ μm), designed to smooth noise while preserving mean gradients. Only the result for *Point 3* will be discussed in the present summary.

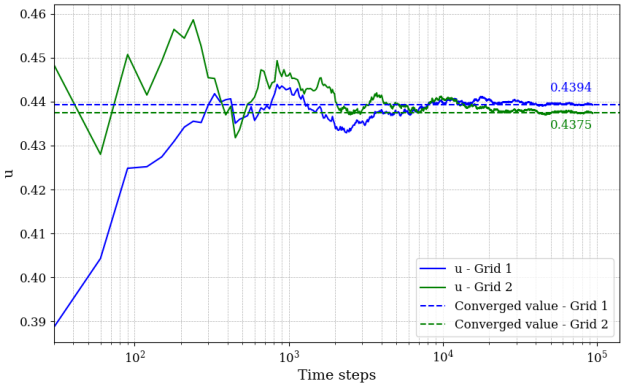

Figure 2: Convergence behavior of u at *Point 3*.

A low positive value for w was noted in the results, suggesting a weak spanwise pressure gradient. This is a very large scale with a long coherence length in the spanwise direction, and it is strongly tightened to the dynamics at the boundaries. There are vortices that may enter the separation region and could generate small areas of recirculation extending in the spanwise direction. This behavior alternates due to counter-rotating vorticity at the junctions, with the inner region exhibiting similar dynamics. However, the streamwise component (see Figure 2) is clearly converged, with a mean deviation that falls below 1% already after 1000 of time steps, and is fully converged after 40000 images.

3.2. Streamwise velocity

Figure 3 illustrates the mean flow structure and velocity fields in the backward-facing ramp ge-

ometry. The ramp (gray) is on the left, with the main flow moving from left to right. The fluid enters from top-left with relatively high momentum. As it encounters the edge, separation occurs generating a shear layer that reattaches farther downstream. The streamwise velocity remains relatively high in the region above the ramp, since the free-stream fluid is largely unimpeded in that zone. In contrast, a recirculation zone is present immediately after the step. Within this bubble, a portion of the fluid near the wall flows upstream relative to the main flow. This upstream motion is sustained by entrainment and momentum transfer from the faster shear layer located above. The reattachment point is subjected to low-frequency "flapping" of the separated shear layer, which can oscillate vertically and horizontally, due to the formation and shedding of large-scale vortices that lie within the wake of the ramp. In a mean sense, the reattachment point was estimated to be at approximately 41.9 mm.

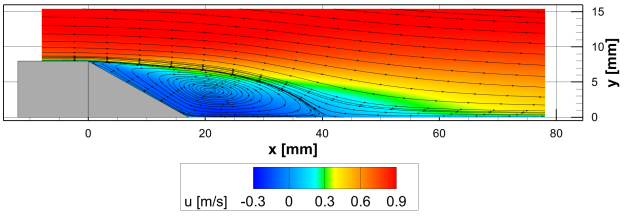

Figure 3: Time and spanwise-averaged u-distribution, with super-imposed streamlines.

3.3. Reynolds stresses

The three Reynolds stresses components in Figure 4 shows a distribution which extends in the free shear layer (from $x \approx 0$ mm to $x \approx 40$ mm) due to the high level of mixing rate. They start from the separation point of the ramp, and quickly increase in both the intensity and width, along the streamwise direction. A peak can be identified at approximately $x = 30$ mm. Instead, they experience a very fast reduction as the shear layer reattaches. A change in shape occurs at approximately $x = 20$ mm, where a kink appears in all three distributions. It is clear that the change in Reynolds stresses behavior coincides with the pressure jump in Figure 5a, with particles exhibiting strong acceleration (blue region of negative velocity in the lower-right part of the recirculation bubble). The recirculating flow is subjected to compression, followed by relaxation closer to the ramp, accompanied by a strong pressure gradient within the flow. Due to the squeezing effect near the wall, the flow accelerates and consequently, turbulence amplitudes are dampened. As soon as the flow opens again, a large increase in turbulence production occurs, altering the Reynolds stresses distributions, so resulting in the observed shape change.

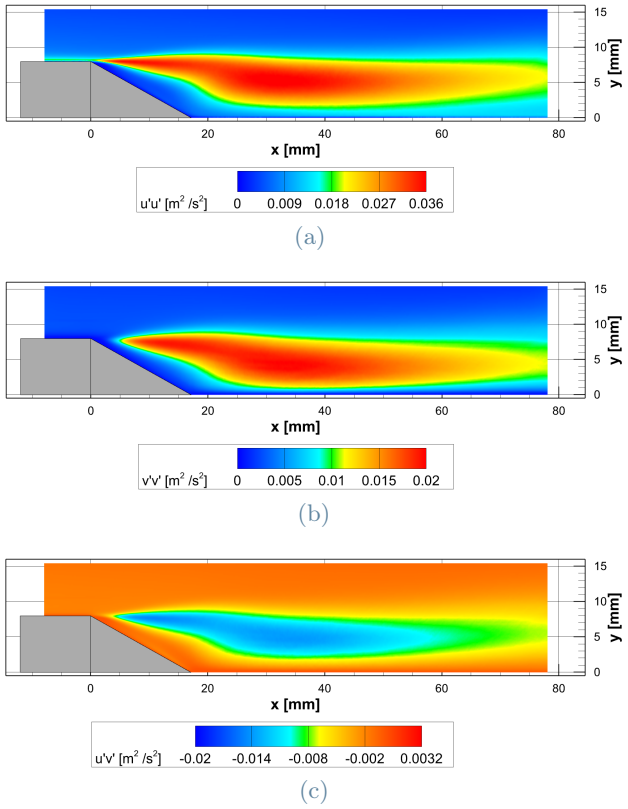

Figure 4: Time- and spanwise-averaged Reynolds stresses distributions. (a) $u'u'$-distribution, (b) $v'v'$-distribution and (c) $u'v'$-distribution

3.4. Accelerations

The time- and spanwise- averaged streamwise and vertical accelerations distribution are shown in Figure 5, and provide a direct interpretation into pressure gradient effects on flow behavior. An initial streamwise acceleration occurs due to the model's presence, followed by a suction peak near the edge, indicating a pressure minimum, which eventually turns into a deceleration as soon as separation occurs. Downstream of the edge, the shear layer is starting to developing and widening vertically, a pressure reduction occurs and the flow starts to accelerate again due to a "squeezing effect" with the

wall below. This is caused by the reduction in flow area as the shear layer interacts with the wall. As soon as the pressure gradient relaxes instead, the flow decelerates and produces the jump shown in Figure 5a. After reattachment further downstream, the flow normalizes to a zero-pressure gradient, with an almost negligible acceleration in the streamwise direction. In the shear layer region, large scale vortices form and convect downstream. This implies that positive or negative peaks reflect the center, in the mean sense, of these turbulent structures.

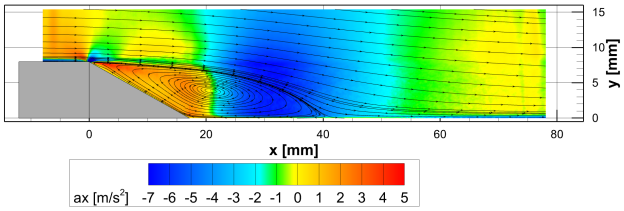

(a)

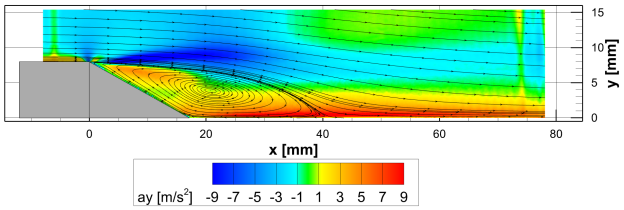

(b)

Figure 5: Time- and spanwise-averaged accelerations distributions.

3.5. Probability density function

With a binning average approach applied to STB results, velocity components are extracted for a specific bin. In this study, a probability density function (PDF) analysis was conducted to examine velocity fluctuation distributions in a point within the shear layer (see Figure 6). The PDF of the instantaneous spanwise velocity is symmetrical about zero, which imply that the flow can be considered as bi-dimensional in the x and y axis. Instead, PDFs of streamwise and wall-normal velocity components reveal slight asymmetries. The asymmetry in the streamwise direction can be attributed to the intermittent nature of high- and low-speed streaks induced by shear layer instabilities. Instead, the wall normal distribution show an imbalance in vertical velocity fluctuations, which is likely caused by the interaction between large-scale vortical structures and the surrounding turbulent flow. The asymmetry in the PDFs may reflect the dominance of certain flow patterns, such as upwash or downwash regions, which result from the coherent structures' dynamics. These are based on the relationship where low-amplitude, spanwise more extended Q4 events are balanced by higher-amplitude but narrower Q2 events (Q2 and Q4 represent the two quadrants of the JPDF of negative $u'v'$-Reynolds stresses). Together, these events contribute to more turbulence than is canceled out by the reverse positive $u'v'$ events in Q1 and Q3.

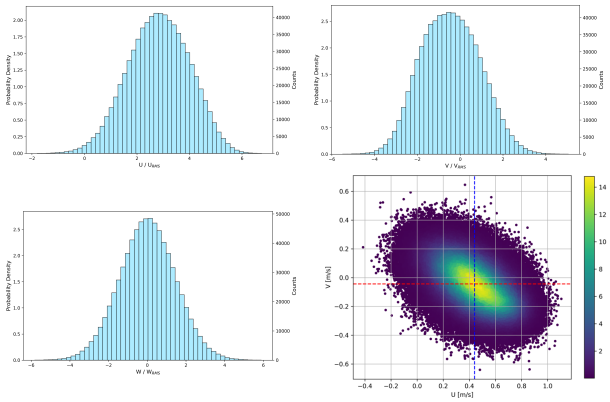

Figure 6: (Top-left) PDF of u. (Top-right) PDF of v. (Bottom-left) PDF of w. (Bottom-right) JPDF of u and v.

3.6. Two-point correlation

The streamwise velocity fluctuation correlation $R_{u'u'}$ reveals an elongated zone of positive correlation stretching downstream, demonstrating the presence of coherent structures. These spanwise alternating high- and low-speed streaks, are aligned by the mean flow in the streamwise direction, reinforcing their coherence and causing a slow decay along the x direction. The correlation of vertical velocity fluctuations $R_{v'v'}$ exhibits a periodic pattern along the streamwise direction, with vortices producing alternating regions of positive and negative correlation. As the vortices travel downstream, they interact with the mean flow and neighboring structures, further amplifying their influence on the shear layer dynamics. The alternating positive and negative correlation zones in $R_{v'v'}$ provide direct evidence of the periodicity induced by KH instabilities, which is the main cause for the unsteadiness of the reattachment length. The correlation of the spanwise velocity fluctuations $R_{w'w'}$ shows alternating regions of positive and negative cor-

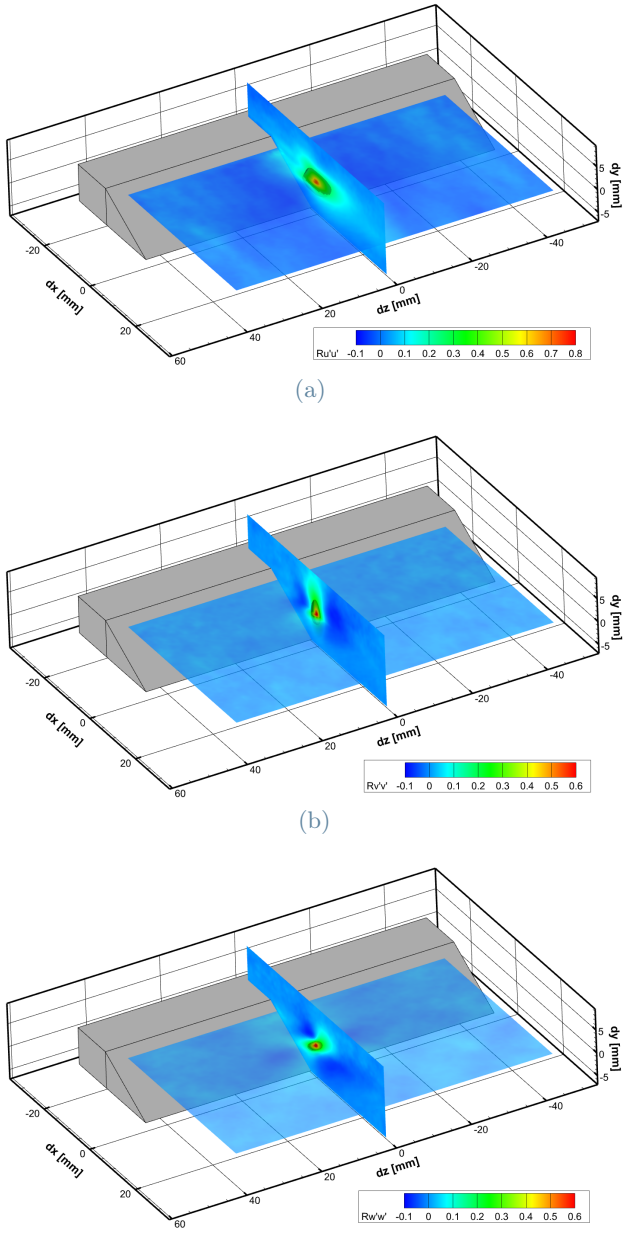

(a)

(b)

(c)

Figure 7: (a) Streamwise velocity correlation. (b) Wall-normal velocity correlation. (c) Spanwise velocity correlation. Isosurfaces at 0.25.

relations, characterized by a symmetric behavior. This pattern is due to the presence of hairpin vortices, which are typical of turbulent shear flows. Hairpin vortices induce spanwise velocity streaks, and alternating regions of positive and negative w' appear on either side of the vortex core. Positive correlations occur on the same side of a vortex and negative correlations on opposite sides. This structured distribution indicates an organized nature of spanwise velocity fluctuations, leading to the characteristic bended peak.

3.7. Residence time analysis

STB allows long trajectories to be established and analyzed for studing the transport properties of fluid elements. The recirculation region was defined by employing two different constraints. Firstly, a spline defined by a set of points, and secondly a constraint on the streamwise velocity $u < 0.35\ m/s$. The results are obtained by averaging the three time-resolved runs.

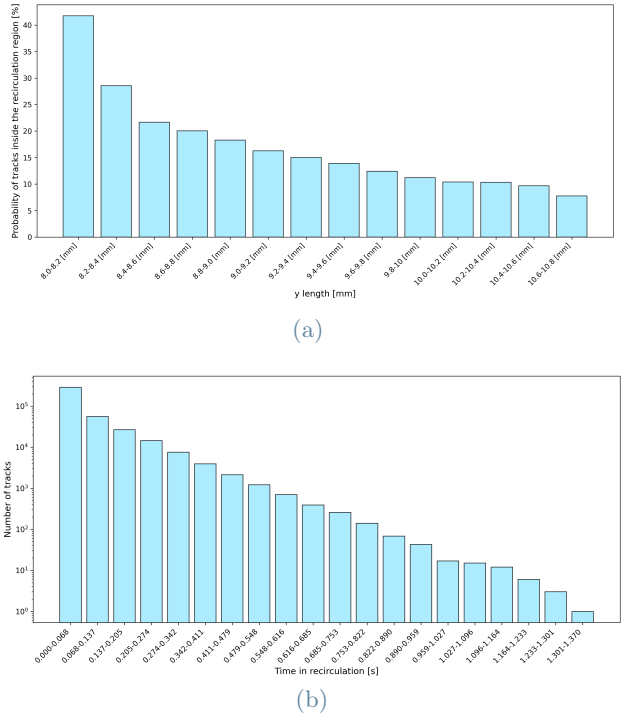

(a)

(b)

Figure 8: (a) Bin-probability a track fall into the recirculation region. (b) Logarithmic bin-distribution of the average time spent within the recirculation bubble.

A preliminary analysis defined the overall number of tracks entering the recirculation region, which is approximately 25%, on an average of 120000 particles tracked simultaneously (only for the lower subvolume). A further study on the local probability is conducted by sizing the wall normal direction before the ramp, dividing in 14 bins of equal size, spanning from 8 mm (ramp position) to 10.8 mm (upper limit for the inner subvolume). The likelihood of a particle track entering the recirculation region decreases as the considered distance in the y-direction increases, with an exponential trend (see Figure 8a). This is attributed to the shear layer, which entrains higher-positioned particles

downstream rather than allowing them to enter the low-momentum recirculation zone. Figure 8b illustrates the average residence time of particles within the recirculation region. The linear trend on the logarithmic scale suggests that the distribution decays exponentially. The longest recorded track spans 4109 frames, corresponding to $t = \frac{4109}{3000} \approx 1.370\ s$, and defines the upper limit of the analysis. The steep decline in particle count for longer residence times indicates that most particles lie within the recirculation zone for a very small time before being spilled out.

4. Conclusions

3D Shake-The-Box was employed to capture the dynamics of a turbulent boundary layer, developed over a flat plate at near-zero pressure gradient, followed by separation over a backward-facing ramp in the *Große Wasserkanal Braunschweig* at $Re = 1.2 \times 10^6$, 1.6×10^6, 2.2×10^6, 2.7×10^6. Results are provided only for $Re = 1.2 \times 10^6$ due to data volume.

A convergence analysis was conducted to assess the impact of time steps on the reliability of flow statistics, using five different points in two different grids. The measurement suffered strong reflections very close to the walls, making the evaluation of the reattachment length quite difficult. The distributions of Reynolds stresses highlight the turbulence mixing that occurs in the free shear layer, with a dampening of fluctuations in the recirculation bubble center. The streamwise acceleration confirms the link between stresses variations and pressure-driven acceleration effects, and represent a novel feature of this dataset. The probability density function of velocities within the shear layer reveals asymmetries in both the streamwise and wall-normal components. A deeper understanding using 3D two point correlation demonstrates the presence of coherent structures influencing the dynamics within the shear layer. The streamwise velocity correlation shows an elongated region of positive correlation, confirming the dominance of streaky structures stretching downstream due to turbulence anisotropy. The wall-normal velocity correlation is characterized by periodic patterns typical of KH instabilities. Instead, alternating positive and negative regions are revealed from the spanwise velocity correlation, reflecting the impact of hairpin vortices on spanwise velocity fluctuations. Finally, a novel analysis is proposed to investigate particle transport properties using the long Lagrangian trajectories. The study reveals that approximately 25% of tracked particles enter the recirculation region, with entry likelihood decreasing exponentially with wall-normal distance upstream of the step. An analysis of averaged time is provided, with the longest recorded trajectory lasting approximately 1.370 s. This approach offers new insights into turbulence-driven transport mechanisms and flow structure interactions, with implications for experimental and numerical modeling. The proposed study offers various opportunities for further studies. By applying a dynamic mode decomposition it would be possible to extend the study to the flapping motion of the shear layer. This would also improve the understanding of reattachment point sensitivity. Space-time correlations could be used to estimate not only the evolution but also the persistence of vortical structures. The application of FlowFit to particles tracks obtained though 3D Shake-the-Box would enable the reconstruction of the time-resolved 3D velocity gradient tensor and pressure fields. Finally, the analysis focused on the lowest Reynolds number. An integration of result from higher flow velocities would provide notable insight, particularly regarding the reattachment length. The same model was also employed in a temperature-sensitive paint measurement campaign, making a quantitative comparison of near wall flow features highly relevant.

References

[1] Cornelia Grabe. Dlr-project adamant: Adaptive, data-driven physical modeling towards border of envelope applications. In DGLR, editor, *DLRK 2022*, 2022.

[2] Daniel Schanz, Sebastian Gesemann, and Andreas Schröder. Shake The Box: Lagrangian particle tracking at high particle image densities. *Experiments in Fluids*, 57(5):70, 2016.